

Conceptual Design and Stability Analysis of a Fixed Wing UAS Research Platform for Aerial Experiments

Ashish Karki ^a, Kamal Darlami ^b, Sudip Bhattra ^c

^{a, b, c} Department of Mechanical and Aerospace Engineering, Pulchowk Campus, IOE, Tribhuvan University, Nepal

Corresponding Email: ^a075msmde004.ashish@pcampus.edu.np, ^bdarlami.kd@pcampus.edu.np, ^csudip@ioe.edu.np

Abstract

Recently, the use of Unmanned Aerial Systems(UAS) in civil applications have been very popular. The UAS technology has also improved considerably. UAS can also be used in number of aerial experiments like air quality measurement and monitoring, aerial sensing,etc. The UAS used in these research are highly limited to the multirotor drones (mainly quadcopters) which poses significant endurance limitation due to their high energy consumption. As an alternative to this problem, a fixed wing UAS design is proposed that can be used as a baseline platform to fly the test equipment onboard and perform the aerial experiments. The conceptual design of the UAS is done analytically. The conceptual design involves takeoff weight estimation, constraint analysis, configuration selection and propulsion system selection. The cruise performance of the aircraft was studied analytically and the stability analysis was done using the low fidelity analysis tools such as XFLR5. The mission specification of the proposed UAS, Conceptual design, performance estimation and Static and dynamic stability of the UAS is presented in this paper.

Keywords

Unmanned Aerial System, Conceptual Design, Constraint Analysis, Wing loading, Power loading, Static Stability, Dynamic Stability

1. Introduction

The use of Unmanned Aerial Systems (UAS) has grown significantly in military missions as well as civil application domains such as real-time monitoring, remote sensing, search and rescue, goods delivery, surveillance and security missions, precision agriculture, civil infrastructure inspection, rescue missions, precision strikes, reconnaissance and surveillance, weather monitoring, wireless coverage etc. Due to its ease of deployment, low acquisition and maintenance costs, great mobility, and ability to hover, small-scale UAS are a viable option for commercial applications [1]. Small scale UAS can be deployed in number of ways such as ordinary runway, using hand or launcher or by using other larger aircrafts. UAS can be utilized in precision agriculture for crop management and monitoring, weed detection, irrigation scheduling, disease detection, pesticide spraying and gathering data from ground sensors (moisture, soil properties, etc.). In agriculture, UAS deployment can be a cost-effective and time saving technology which can help for improving crop yields,

farms productivity and profitability in farming systems [2].

Also for atmospheric measurements, for example air quality monitoring, small and lightweight UAS can provide more accurate information on aerosol distribution throughout the atmospheric column, which is needed to better understand air quality and composition in specific atmospheric layers [3]. UAS can cover large areas and can be remotely deployed to access difficult and dangerous areas. Hence, UAS poses better operational flexibility than land based methods for pollution monitoring as well.

The UAS can also operate in areas of emergency service like disaster management. Currently, the research and experiment involving UAS in these application areas is hugely limited to multi rotor drones. The multi rotor UAS does not consider the stable operation of the vehicle under environmental disturbance such as gusts [4] and also these multi rotor drones faces the short endurance limitation and payload capacity limitations due to their high energy consumption. This shortcoming can be overcome by using fixed wing alternatives. Unlike multi-rotor

drones, fixed wing aircraft has very low thrust to weight ratio and high lift to drag ratio which enable it to fly for longer time with less power requirement. Fixed wing UAS having BWB configuration has very high aerodynamic efficiency but has extra demerit of complex control and stability design due to the absence of horizontal stabilizers [5]. Fixed wing aircraft are typically capable of covering greater area over a given time interval and offers flexibility in terms of endurance and payload capacity whereas they loose in terms of capability to hover at single point and ease to takeoff or land. But, they can be designed and built to be inherently stable, compact and easy to transport and deploy, allowing them to operate in remote regions with minimal infrastructure.

2. Problem Statement

2.1 Mission Specification

The proposed fixed wing UAS is a test platform designed to fly the test equipment on board. It has maximum takeoff weight of 10.0 ± 1.0 kg, with the maximum payload capacity of 2.5–3.0 kg by weight and about 6750 cm^3 by volume. The UAS will be mainly capable of performing two mission cruising at two different altitude. The design speed requirement of the UAS set initially are 12 m/s stall speed, takeoff at 15 m/s and cruise at 25 m/s.

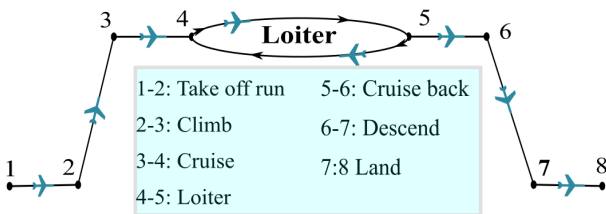


Figure 1: Mission Profile of the proposed UAS

The UAS is capable of cruising at 1000 ft above ground level (AGL) i.e. 5000 ft above mean sea level (AMSL). This low-altitude mission has flight endurance requirement of about 60 minutes carrying maximum payload weight. High altitude mission takes place at 2000 ft AGL i.e. 6200 ft AMSL. During this mission, aircraft has flight endurance time of about 120 minutes with maximum payload weight. The schematic diagram of different flight phases during the specified mission is illustrated in figure 1.

3. Conceptual Design

The Conceptual design is first and foremost step in aircraft design procedure. It mainly involves decision making and selection process rather than calculation. The general design requirement is entered into the process to generate the satisfactory configuration. The design requirement taken into consideration are maximum takeoff weight, wing loading and power requirement. These parameter affects the takeoff performance, climb performance, cruise performance, turn performance and stall speed [6]. The final output of the conceptual design is three orthographic view of the aircraft that represents the aircraft configuration.

3.1 Takeoff Weight Estimation

The total takeoff weight can be estimated by grouping weight into its constituent sub-systems and the weight of the subsystems are individually calculated using historical and commercially available data [7]. The subsystem in UAS are: structures, actuators and instruments, avionics, powerplant, and test equipment as payload. The structural weight, actuators, instruments constitutes the empty weight while payload weight includes components like avionics, camera, test equipments, etc. The empty weight of the aircraft can be estimated by power law relation (equation 1) based on gross takeoff weight [8].

$$W_{empty} = A \cdot W_{takeoff}^B \tag{1}$$

Other component weight can be found on the specification sheet or datasheet of the respective component. The gross takeoff weight of the aircraft is obtained by adding all of these sub-system weight.

$$W_{t/o} = W_{empty} + W_{payload} + W_{powerplant} \tag{2}$$

Table 1 presents the component wise classification of weight groups.

Weight Group	Weight (gram)	Components
Avionics	275	IMU Flight controller, GPS, ESC, wires, etc.
Powerplant	1500	Motor propeller battery
Structure	6000	Wing, tail, boom, fuselage, landing gear
Actuators	200	Servo motors linkages
Instruments	200	Barometer, velocity sensor
Total Empty Weight	8175	
Payload	2500	Test equipment
Gross Takeoff Weight	10675	

Table 1: Component wise weight distribution

3.2 Constraint Analysis

Constraint analysis allows to determine the feasible region in wing loading (W/S) versus the power loading (P/W) plot or sometimes Thrust Loading (T/W) plot [9, 10]. The design space is the region in the plot which satisfies all the constraints and the starting design point lies in this space. The preliminary design process starts from the design point. Constraint analysis simplifies the selection of wing area and propulsion system. The design constraints set to get this initial design point are :

1. Stall speed requirement
2. Maximum rate of climb
3. Take off run
4. Cruise requirement

The result of constraint analysis is power loading plot against wing loading for these different flight phases and is shown in figure 2.

3.3 UAS Configuration

The UAS configuration largely depends on operational requirement of the UAS. Further, Manufacturing requirements, Stability requirements also affect the configuration. The tail configuration type is mainly defined by the trim requirement of the aircraft [11]. The twin boom UAS allow attaching and

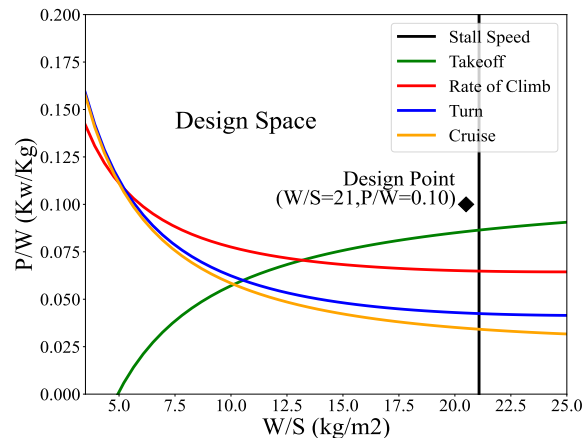


Figure 2: Constraint analysis

disconnecting the tail, which makes the design highly modular and easily manufacturable. In Mini-UAS like these, the two major components whose configuration needs to be selected are wing and tail.

Wing Configuration Due to operational and manufacturing requirements, a straight taper wing with trailing edge sweep of about 9° is made. Table 2 presents specification of the wing.

Wing Specification	
Wing Span	2.5 m
Wing Area	0.61 m ²
Wing Load	14.653 kg/m ²
Aspect Ratio	10.2
MAC	0.26 m
Taper Ratio	0.44
Root to Tip Sweep	-2.18 °
XNP	0.172 m

Table 2: Wing specification table

Tail Configuration To fulfill the trim requirements of the aircraft, number of tail configurations like conventional type, T-tail type, V-tail type, Y-tail type, H-tail type, etc.[6] are available. The configuration that is more often employed in the Remotely Piloted Aircraft Systems (RPAS) such as the Northrop Grumman Global Hawk or the General Atomics MQ-9 Reaper is the V-tail configuration[12]. V-tail configuration are also widely used configuration in civil application Twin-boom UAS [13, 14].

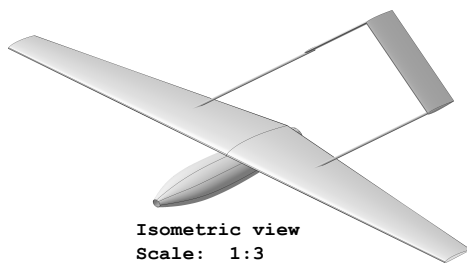


Figure 3: conceptual design of proposed UAS

Propulsion System To size the propulsion system, the constraint analysis done before was referred. The power and thrust required in every flight phases is calculated and figure 2 shows that the main power plant constraint is posed by takeoff requirement. The UAS requires maximum power during the take-off phase. Hence, the propulsion system needs to be selected fulfilling this take-off power requirement. An electric Brushless motor AT 4120 coupled with APC 15×8 satisfies this power requirement and is recommended propulsion system for this UAS. The puller type propulsion system with motor and propeller mounted aft of the fuselage between the two booms is favorable due to the center of gravity and space requirements.

3.4 Performance Evaluation

To know the performance characteristics, the power available from suggested propulsion system at different altitude and power required to fly at different altitude is calculated using the basic flight dynamics equation in cruise [15]. As air density decreases with increase in altitude, the thrust generated also lowers than that of the sea level. Figure 2 shows the plot of power available and power required at different altitude against the flight velocities. The maximum flight ceiling of the UAS is about 50,000 ft. Also, The UAS can fly at both operating altitude suggested in mission specification with the maximum velocity of 50 m/s and 55 m/s. Since, the minimum velocity seen from the graph is lower than the stall velocity, Stall speed is the lowest possible velocity for the aircraft at both operating altitude.

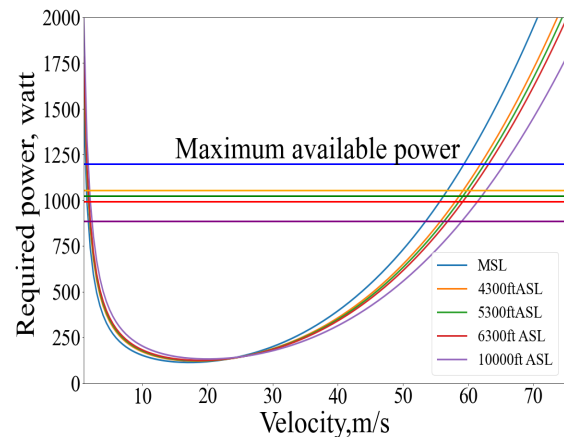


Figure 4: Power required to fly at different altitude and velocity

4. Stability Analysis

Stability of the aircraft is the property of its equilibrium state and is studied under two aspects: Static Stability and Dynamic Stability. To study both of these stability, the UAS model is recreated in XFLR5. XFLR5 allows to analyse the airfoils and wings operating at low Reynolds number using Lifting Line Theory (LLT) and Vortex Lattice Method (VLM). Stability of the aircraft in all three direction, longitudinal, lateral and directional, is assessed using XFLR5.

4.1 Static Stability

Static Stability is the tendency of the vehicle, which after disturbance, returns or tends to return to its original equilibrium from which it was disturbed. The results of Static Stability analysis in XFLR5 is presented in terms of graphs of pitching moment against angle of attack (figure 5), rolling moment against sideslip angle (figure 6) and yawing moment against sideslip angle (figure 7).

The UAS is statically stable in longitudinal direction with static margin of about 20% and is also stable directionally. However, the lateral stability, also called roll stability of the aircraft is compromised as the wing does not have dihedral angle or sweep as it poses operational and manufacturing difficulties.

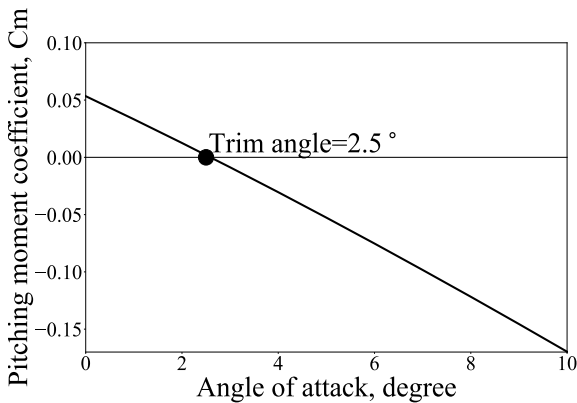


Figure 5: Pitching moment curve

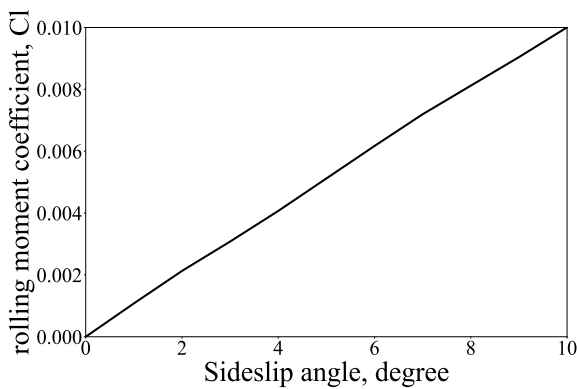


Figure 6: Rolling moment curve

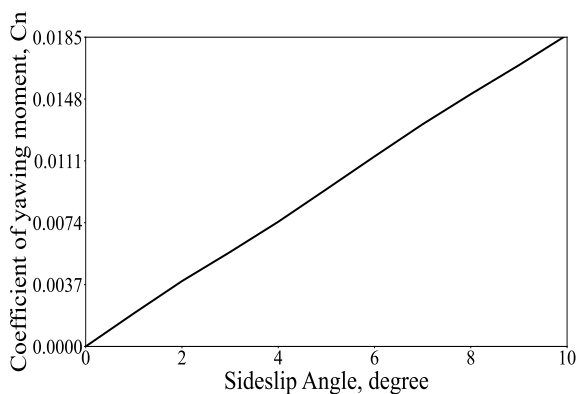


Figure 7: Yawing moment curve

4.2 Dynamic Stability

Dynamic stability studies the time history of the motion of the aircraft after it is disturbed from the equilibrium position. The roots of the characteristic equation of the equation of motions are calculated, which represents five modes of oscillation: two in the longitudinal direction and three in the lateral direction.

4.2.1 Longitudinal Modes

From XFLR5 computation, the longitudinal state matrix and the characteristic roots are obtained as equation 3 and 4 respectively.

$$A_{long} = \begin{bmatrix} -0.0243 & 0.2436 & 0 & -9.81 \\ -0.7763 & -4.4294 & 24.2029 & 0 \\ -0.0024 & -1.4096 & -4.0071 & 0 \\ 0 & 0 & 1 & 0 \end{bmatrix} \quad (3)$$

$$\lambda_{1,2} = 4.228 \pm 5.843i$$

(4)

$$\lambda_{3,4} = -0.002741 \pm 0.452i$$

Short-Period Mode This mode is excited due to the symmetrical disturbances in pitch angle and the angle of attack due to upward gust or step elevator input. The roots $\lambda_{1,2}$ represents this mode showing that the aircraft is highly stable with natural frequency 0.93 Hz and damping ratio of 0.586. The disturbances in terms of forward speed, downward velocity, pitch rate and pitch angle are damped rapidly under 1–2 seconds. Figure 8 shows the pitch angle damping in short period mode of the aircraft.

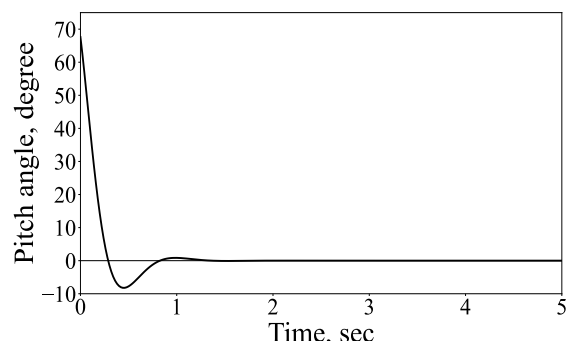


Figure 8: Pitch damping in short period mode

Phugoid Mode Phugoid mode is slowly damped sinusoidal motion which exhibits when the aircraft

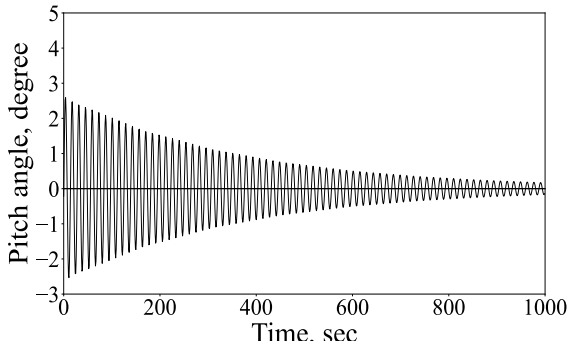


Figure 9: Pitch damping in phugoid mode

has to pitch up suddenly bleeding some of its speed. Under phugoid mode, the aircraft goes to the saw-tooth motion continuously but the angle of attack remains constant. The two roots $\lambda_{3,4}$ represents the phugoid mode and it was observed that it takes about 4-5 minutes to dampen out the disturbances in phugoid mode. As seen in figure 9, response of the aircraft in phugoid mode is very lightly damped and has very high frequency. The phugoid mode occurs so slowly that the operator or autopilot can easily negate the disturbance by small control inputs [16].

4.2.2 Lateral Stability

The lateral state matrix and the characteristic roots obtained in lateral direction are presented in equation 5 and 6 respectively.

$$A_{lat} = \begin{bmatrix} -0.2365 & 0.0274 & -24.9894 & 9.81 \\ 0.5577 & -10.1419 & 1.8769 & 0 \\ 0.6869 & 0.3714 & -0.9349 & 0 \\ 0 & 1 & 0 & 0 \end{bmatrix} \quad (5)$$

$$\lambda_1 = -13.47$$

$$\lambda_{2,3} = -1.607 \pm 8.125i \quad (6)$$

$$\lambda_4 = 0.03495$$

Roll Subsidence mode The root λ_1 is associated with roll subsidence mode. This mode is highly damped. The time taken to damp the roll disturbance is less than a second. Figure 10 is the time response of the aircraft in roll subsidence mode.

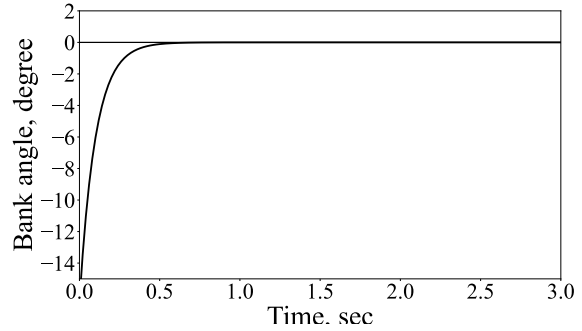


Figure 10: Bank angle damping in roll subsidence mode

Dutch-Roll Mode Dutch-Roll mode exhibits when the aircraft's bank angle or heading is suddenly disturbed from the equilibrium position due to gust. This mode is combination of both rolling and yawing motion and is oscillatory in nature. The roots $\lambda_{2,3}$ represents the dutch roll motion. This mode is damped with natural frequency of 0.656 hz and damping ratio of 0.147. The dutch-roll disturbances (sideslip velocity, roll rate, yaw rate and bank angle) recover back to the equilibrium in about 5 seconds. Figure 11 shows the bank angle damping of the aircraft in dutch-roll oscillation.

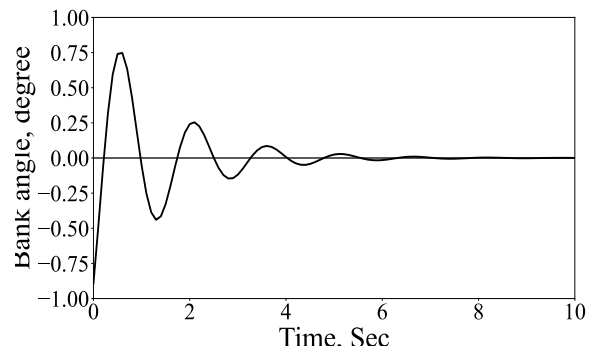


Figure 11: Dutch roll damping

Spiral Mode The positive real root λ_4 represents the spiral mode, which is divergent. This mode is exhibited when an aircraft is banked to a very high bank angle and then left stick free. The time taken by the aircraft to double the amplitude of disturbance (sideslip velocity, roll rate, yaw rate and bank angle) is about 6.5 seconds. Figure 12 shows the rolling rate divergence in spiral mode.

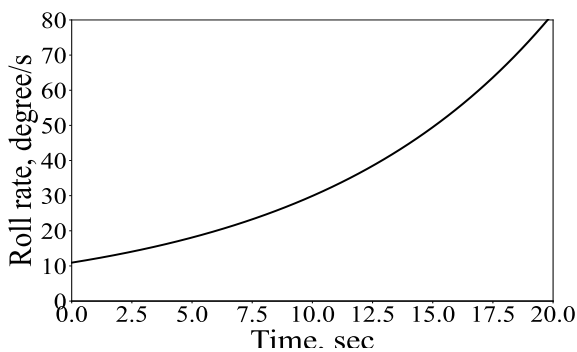


Figure 12: Rolling rate divergence in spiral mode

5. Conclusion

To address the need of fixed wing UAS that mainly serves as a test platform to conduct aerial experiments a light aircraft was designed and its stability is studied using XFLR5. The UAS can also be used in different application areas like surveillance, air quality measurements, precision agriculture, mapping, etc. conceptual and preliminary design of the UAS with propulsion system capable of performing the specified mission is proposed. The power constraint of the UAS is defined by the takeoff run. Decreasing the takeoff run will allow the UAS to fly with smaller and lighter power-plant. The vehicle is stable longitudinally and directionally. The lateral stability of the aircraft is trade off with the manufacturing and operational simplicity. The dynamic modes are convergent except spiral mode, which can be divergent for UAS like these. The high frequency oscillation in phugoid mode can be controlled manually or with an autonomous flight controller. The fixed wing UAS are promising alternatives to multi-rotor UAS in terms of payload capacity and endurance. The future work includes flight simulation and experimental test to compare the numerical results obtained.

References

- [1] Samira Hayat, Evşen Yanmaz, and Raheeb Muzaffar. Survey on unmanned aerial vehicle networks for civil applications: A communications viewpoint. *IEEE Communications Surveys & Tutorials*, 18(4):2624–2661, 2016.
- [2] Hazim Shakhathreh, Ahmad H Sawalmeh, Ala Al-Fuqaha, Zuochoao Dou, Eyad Almaita, Issa Khalil, Noor Shamsiah Othman, Abdallah Khreishah, and Mohsen Guizani. Unmanned aerial vehicles (uavs): A survey on civil applications and key research challenges. *Ieee Access*, 7:48572–48634, 2019.
- [3] Tommasofrancesco Villa, Felipe Gonzalez, Branka Miljevic, Zoran D. Ristovski, and Lidia Morawska. An overview of small unmanned aerial vehicles for air quality measurements: Present applications and future prospectives. *Sensors (Switzerland)*, 16(7):12–20, 2016.
- [4] Saleen Bhattarai, Kushal Poudel, Nishant Bhatta, Sanjaya Mahat, Sudip Bhattarai, and Kaman S Thapa Magar. Modeling and development of baseline guidance navigation and control system for medical delivery uav. In *2018 AIAA Information Systems-AIAA Infotech@ Aerospace*, page 0508. 2018.
- [5] Sanjiv Paudel, Shailendra Rana, Saugat Ghimire, Kshitiz Kumar Subedi, and Sudip Bhattarai. Aerodynamic and stability analysis of blended wing body aircraft. *International Journal of Mechanical Engineering and Applications*, 4(4):143–151, 2016.
- [6] Daniel Raymer. *Aircraft Design: A Conceptual Approach, Sixth Edition and RDSwin Student SET*. 2019.
- [7] Jay Gundlach. *Designing Unmanned Aircraft Systems: A Comprehensive Approach, Second Edition*. American Institute of Aeronautics and Astronautics, Inc., 2014.
- [8] Dries Verstraete, Jennifer L. Palmer, and Mirko Hornung. Preliminary sizing correlations for fixed-wing unmanned aerial vehicle characteristics. *J. Aircr.*, 55(2):715–726, 2018.
- [9] Andrew J. Keane, Andras Sobster, and James P. Scanlan. *Small Unmanned Fixed-Wing Aircraft Design*. 2017.
- [10] Nikolajs Glīzde. Wing and Engine Sizing by Using the Matching Plot Technique. *Transport and Aerospace Engineering*, 5(1):48–59, 2018.
- [11] Mohammad H. Sadraey. *Aircraft Design*. John Wiley & Sons, Ltd Registered, 2013.
- [12] Alejandro SANCHEZ-CARMONA and Cristina CUERNO-REJADO. Vee-tail conceptual design criteria for commercial transport aeroplanes. *Chinese Journal of Aeronautics*, 32(3):595–610, 2019.
- [13] P. D. Bravo-Mosquera, A. Martins-Abdalla, H. D. Ceron-Muñoz, and F. M. Catalano. Conceptual and aerodynamic design of a UAV for superficial volcano monitoring. *30th Congress of the International Council of the Aeronautical Sciences, ICAS 2016*, 2016.
- [14] P Panagiotou, P Kaparos, C Salpingidou, and K Yakinthos. Aerodynamic design of a male uav. *Aerospace Science and Technology*, 50:127–138, 2016.
- [15] Bandu N Pamadi. *Performance, stability, dynamics, and control of airplanes*. Aiaa, 2004.
- [16] Robert C Nelson et al. *Flight stability and automatic control*, volume 2. WCB/McGraw Hill New York, 1998.